NASA TN D-1551

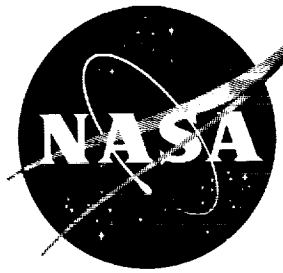

TECHNICAL NOTE

D-1551

THE MAGNETIC FIELD OF A LINE CURRENT IN A TRANSVERSE RAREFIED PLASMA STREAM

By Albert G. Munson

Ames Research Center
Moffett Field, Calif.

NATIONAL AERONAUTICS AND SPACE ADMINISTRATION

WASHINGTON February 1963

Copy 1

Code 1

NATIONAL AERONAUTICS AND SPACE ADMINISTRATION

TECHNICAL NOTE D-1551

THE MAGNETIC FIELD OF A LINE CURRENT IN A TRANSVERSE RAREFIED PLASMA STREAM

By Albert G. Munson

SUMMARY

The steady-state flow of an infinitely conducting, rarefied, neutral plasma past a line current is considered. According to the Chapman-Ferraro theory, the plasma is confined to the exterior and the magnetic field to the interior of a cavity, the boundary of which is a thin current sheath. Within these restrictions the problem is solved exactly by a method similar to the hodograph method of incompressible fluid dynamics, and the magnetic field inside the cavity is presented. The boundary so obtained agrees with that previously given by Hurley who used a different method. Also, the magnetic field inside the cavity is determined by means of an approximate solution for the cavity shape previously obtained by Ferraro. Results of the approximate and exact solutions are compared.

INTRODUCTION

Chapman and Ferraro, in studies of the connection between solar activity and geomagnetic storms, have considered the idealized problem of a rarefied neutral plasma stream interacting with a permanent magnetic field. Under these conditions the permanent field does not penetrate the plasma but has the effect of producing a hollow or cavity in the plasma. The steady-state formulation of this problem is summarized by Dungey (ref. 1). Several investigators have applied this formulation to the interaction of a plasma with a two-dimensional dipole (refs. 2, 3, 4).

The recent evidence that a ring current flows in the magnetosphere has given impetus to the study of the interaction of a plasma with a two-dimensional line current (see ref. 5). Ferraro (ref. 6) and Hurley (ref. 7) have initiated such studies recently. The former obtained an approximate expression for the boundary between the stream and the magnetic field, and the latter an exact one. The present paper applies the formulation of Hurley and Ferraro to the exact and approximate magnetic fields inside the cavities. Inasmuch as the approximate formulation of Ferraro has been applied to three-dimensional problems by Beard (ref. 8), and Spreiter and Briggs (ref. 9), extensive comparisons of the exact and approximate solutions are made.

FORMULATION OF THE PROBLEM

It is considered (ref. 1) that the particles in the stream travel up to the boundary of the hollow in straight lines and are in effect reflected specularly. In so doing, each particle imparts to the surface twice its normal component of momentum. This change in momentum is balanced by the magnetic pressure at the boundary surface. One thus obtains

$$\frac{H_s^2}{8\pi} = p_o \cos^2\alpha \tag{1a}$$

$$p_o = 2mnv^2 \tag{1b}$$

where H_s is the total magnetic field at the boundary surface; m, n, and v are the mass, number density, and velocity of the positive ions in the undisturbed stream; and α is the angle between the stream and the normal to the surface as shown in figure 1. Because no part of the surface may be shielded from the stream, cos α must lie between zero and unity.

The condition that the magnetic field does not penetrate the plasma means that at the boundary surface the magnetic field must be tangent to the surface, that is,

$$\frac{dy}{dx} = \frac{H_y}{H_x} \tag{2}$$

where x and y are two-dimensional rectangular Cartesian coordinates (see fig. 1) and H_x and H_y are the x and y coordinates of the magnetic field.

The equations to be satisfied inside the cavity are:

$$\frac{\partial H_x}{\partial x} + \frac{\partial H_y}{\partial y} = 0 \tag{3}$$

and

$$\frac{\partial H_y}{\partial x} - \frac{\partial H_x}{\partial y} = 0 \tag{4}$$

The field components must approach the appropriate values at the line current, that is,

$$H_x \rightarrow -\frac{2I_y}{r^2} \tag{5a}$$

$$H_y \rightarrow \frac{2I_x}{r^2} \tag{5b}$$

where $r^2 = x^2 + y^2$ and I is the current carried by the wire. In the above the current is considered to flow out of the paper, and is measured in abamps, and the field is measured in gauss.

THE EXACT SOLUTION

Predictions as to the nature of the physical problem can be made once equations (3) and (4) have been solved subject to the boundary conditions of equations (1), (2), and (5) (with the restriction that $\cos \alpha$ is greater than zero). The main difficulty in obtaining a solution to the equations in their present form is that conditions (1) and (2) must be satisfied on an unknown boundary. To state this another way, the boundary must be determined so that (1) and (2) are both satisfied on it. It will now be shown that, when independent and dependent variables are interchanged, the boundary becomes known. Before this is done, however, it is convenient to introduce a potential function.

If we introduce the complex function W, that is,

$$W = \Phi + i\psi$$

where Φ is a potential function and ψ a stream function, and define

$$H_x = \frac{\partial \Phi}{\partial x} = \frac{\partial \psi}{\partial y} \tag{6a}$$

$$H_y = \frac{\partial \Phi}{\partial y} = -\frac{\partial \psi}{\partial x} \tag{6b}$$

equations (3) and (4) become

$$\frac{\partial^2 \Phi}{\partial x^2} + \frac{\partial^2 \Phi}{\partial y^2} = 0 \tag{7a}$$

$$\frac{\partial^2 \psi}{\partial x^2} + \frac{\partial^2 \psi}{\partial y^2} = 0 \tag{7b}$$

Equations (6) are recognized to be the Cauchy-Riemann equations; thus W is an analytic function of the complex variable $z = x + iy$ (see ref. 10). Similarly, equations (3) and (4) are the Cauchy-Riemann equations for the complex function $H^* = H_x - iH_y$, and H^* is also an analytic function of the complex variable z. Equations (7) can be combined into

$$\frac{\partial^2 W}{\partial x^2} + \frac{\partial^2 W}{\partial y^2} = 0 \tag{8}$$

A result of complex function theory which can be shown by direct substitution (making use of eqs. (3), (4) and (6)) is that if x and y are replaced by H_x and H_y, equation (8) becomes

$$\frac{\partial^2 W}{\partial H_x^2} + \frac{\partial^2 W}{\partial H_y^2} = 0 \tag{9}$$

The boundary conditions, equations (1) and (2), will now be combined into a single relation involving only the component of the magnetic field. From figure 1

$$-\cot \alpha = \frac{dy}{dx} = \frac{H_y}{H_x} \tag{10}$$

Alternatively,

$$\cos \alpha = \frac{H_y}{\sqrt{H_x^2 + H_y^2}} \tag{11}$$

Substituting into equations (1) and simplifying, we have

$$H_x^2 + H_y^2 = \pm(8\pi p_o)^{1/2} H_y \tag{12}$$

where the positive sign is chosen because H_y is always positive on the boundary. Equation (12) then becomes

$$H_x^2 + [H_y - (2\pi p_o)^{1/2}]^2 = 2\pi p_o \tag{13}$$

This is the equation of a circle as shown in figure 2. The condition stated in equation (5) can be expressed in terms of W and the magnetic field as follows. Near the wire

$$W \rightarrow -2iI \log z \tag{14}$$

where I is the current carried by the wire. Equation (5) in complex notation is

$$H^* \rightarrow -\frac{2iI}{z} \tag{15}$$

Substituting into (14) we have, for large H^*

$$W \rightarrow 2iI \log \frac{iH^*}{2I} \tag{16}$$

The boundary value problem has now been transferred into a fixed boundary value problem. It is now necessary to seek a solution to equation (9) which will satisfy the condition that the field is tangent to the curve given by equation (13) and will satisfy (16) for large H^*. It will be recognized that this is analogous to a circular flow which at infinity approaches a vortex flow.

It seems desirable, before obtaining this solution, to point out aspects of the method which apply to other two-dimensional problems. For any enclosed current system, such as a dipole, a relation, such as equation (16), can be obtained relating the magnetic field to the complex potential W. Equation (13) applies to any two-dimensional problem to which (1) and (2) apply. In more complicated problems, however, it is not possible to choose a single sign in this equation as was done above. The boundary therefore becomes a circle plus arcs of another circle. Thus any two-dimensional problem can be reduced to a fixed boundary value problem in the "magnetic" plane. It may happen, however, that the mapping from the physical plane to the magnetic plane is not one to one; that is, two or more points in the physical plane may map into the same point in the magnetic plane.

The solution to the present problem can now be written by analogy with vortex flow, that is,

$$W = 2Ii \log \left[\frac{iH^* - (2\pi p_o)^{1/2}}{2I}\right] \tag{17}$$

Since

$$\frac{dW}{dz} = H^* \tag{18}$$

an expression involving only W and z can be obtained by solving equation (17) for H^*, equating this to $\frac{dW}{dz}$, and integrating. The result is

$$z = \frac{4I}{(8\pi p_o)^{1/2}} \log \left[1 + \frac{(8\pi p_o)^{1/2}}{4I} e^{i \frac{W}{2I}} \right] \tag{19a}$$

or, separated into real and imaginary parts,

$$x + iy = \frac{4I}{(8\pi p_o)^{1/2}} \log \left\{ \left[1 + \frac{(8\pi p_o)^{1/2}}{4I} e^{-\frac{\Psi}{2I}} \cos \frac{\Phi}{2I} \right]^2 + \left[\frac{(8\pi p_o)^{1/2}}{4I} e^{-\frac{\Psi}{2I}} \sin \frac{\Phi}{2I} \right]^2 \right\}$$

$$+ i \frac{4I}{(8\pi p_o)^{1/2}} \tan^{-1} \frac{\frac{(8\pi p_o)^{1/2}}{4I} e^{-\frac{\Psi}{2I}} \sin \frac{\Phi}{2I}}{1 + \frac{(8\pi p_o)^{1/2}}{4I} e^{-\frac{\Psi}{2I}} \cos \frac{\Phi}{2I}} \tag{19b}$$

Since lines of constant Ψ are field lines, they can be determined if particular values of Ψ are chosen and z is calculated for various values of Φ. In particular, the open field line, which is the boundary, can be determined from

$$\frac{(8\pi p_o)^{1/2}}{4I} e^{-\frac{\Psi}{2I}} = 1 \tag{20a}$$

since this produces a curve that approaches infinity in the negative x direction. Substitution of (20a) into (19) leads to

$$\frac{(8\pi p_o)^{1/2}}{4I}(x + iy) = 8 \log\left(\cos\frac{\Phi}{4I}\right) + i\frac{\Phi}{4I} \tag{20b}$$

This is identical to the boundary previously determined by Hurley (ref. 7). The value of the field function at the nose of the boundary (and indeed on the complete boundary) is from equation (20a)

$$\psi_N = -2I \log \frac{4I}{(8\pi p_o)^{1/2}} \tag{21a}$$

The difference in the values of ψ associated with two field lines represents the magnetic flux passing between them. Therefore the flux passing between any field line and the boundary is

$$\bar{\psi} = \psi - \psi_N \tag{21b}$$

An expression for the components of the magnetic field can be obtained by inverting equation (17). The result is

$$H_x + iH_y = 2(8\pi p_o)^{1/2}\left\{\frac{-\sin\frac{\Phi}{2I}}{\frac{(8\pi p_o)^{1/2}}{4I}e^{-\frac{\psi}{2I}}} + i\left[\frac{\cos\frac{\Phi}{2I}}{\frac{(8\pi p_o)^{1/2}}{4I}e^{-\frac{\psi}{2I}}} + 1\right]\right\} \tag{22}$$

The field lines are plotted in figure 3. The variation of the absolute value of the magnetic field is indicated by means of ticks. The direction of the field is, of course, tangent to the field line. Coordinates of the field lines and components of the magnetic field are given in table I. It was convenient to use stretched polar coordinates, that is,

$$\bar{r} = \left(\frac{\pi p_o}{2I^2}\right)^{1/2}(x^2 + y^2)^{1/2} \tag{23a}$$

$$\theta = \tan^{-1}\frac{y}{x} \tag{23b}$$

The components of the magnetic field are expressed as:

$$H_{\bar{r}} = H_x \cos\theta + H_y \sin\theta \tag{24a}$$

$$H_\theta = -H_x \sin\theta + H_y \cos\theta \tag{24b}$$

THE APPROXIMATE SOLUTION

If the equation of the boundary field line is known, the problem of determining the magnetic field inside the hollow becomes a fixed boundary-value problem; that is, the boundary conditions can be applied on a curve known beforehand. If an approximate boundary is known, it can be used to obtain an approximate solution to the problem. It is reasonable to suppose that if the approximate boundary is close to the actual boundary, the approximate field lines will be reasonably close to the actual field lines.

Ferraro (ref. 7) obtained an approximate boundary by assuming that the total field at the boundary is equal to $2f$ times the component of the magnetic field of the wire parallel to the boundary. He then used equation (1) to relate the known magnetic field to the slope of the boundary. This led to a differential equation for the boundary shape. Ferraro's solution is

$$\xi = \eta \cot \eta \tag{25a}$$

where

$$\xi = \frac{x}{r_o} \tag{25b}$$

$$\eta = \frac{y}{r_o} \tag{25c}$$

$$r_o^2 = \frac{2I^2 f^2}{\pi p_o} \tag{25d}$$

and p_o is given by equation (1b). Ferraro, in his original development, set p_o equal to one half the value given in (1b). For a discussion of this point see reference 9. Ferraro then determined f by requiring that the magnetic field just outside the nose of the hollow be zero. (Since the boundary is approximate, the field everywhere outside the hollow cannot be set to zero.) He found that $f = 0.68$ approximately. It is convenient in the present case to determine f so that the approximate boundary matches the exact one at the nose. This gives

$$f = 0.6931 \tag{26}$$

We now regard the boundary as known and proceed to calculate the field inside it. The differential equation for the field lines is

$$\frac{dy}{dx} = \frac{H_y}{H_x} \tag{27}$$

If the components of the magnetic field are known, this equation can be integrated to determine the coordinates of the field lines. The components

can be determined in two ways since two boundary conditions exist for the exact problem. The first is equation (1) which specifies the value of the field on the boundary. The other is equation (2) which specifies that the normal component of the field vanishes on the boundary. Associated with the given approximate boundary and each of these conditions is a unique set of field lines. Therefore two different sets of field lines can be computed inside the approximate hollow. As mentioned earlier, Ferraro used equation (1) to determine his approximate boundary. It is therefore more consistent to use equation (1) in conjunction with Ferraro's boundary to determine the field lines. The magnetic field is made up of the field caused by the current flowing in the wire and that caused by the currents flowing in the bounding surface. The currents flowing in the sheet can be determined by applying equation (1). Since the magnetic field outside the sheet is zero (nearly zero in the approximate case) and is equal to $(8\pi p_o)^{1/2} \cos \alpha$ just inside the sheet, the currents flowing must be such as to produce a jump of this magnitude in the magnetic field, that is,

$$j = \frac{H_s}{4\pi} = -\sqrt{\frac{p_o}{2\pi}} \cos \alpha = -\frac{If}{\pi r_o} \cos \alpha \tag{28}$$

where j is the current per unit length of the sheet. The Biot-Savart law can now be used to obtain a relation for the magnetic field induced by these currents. The result is

$$H_{x_1} = \frac{2If}{\pi r_o} \int_{-\pi r_o}^{\pi r_o} \frac{y - y'}{(x - x')^2 + (y - y')^2} \, dy' \tag{29a}$$

$$H_{y_1} = -\frac{2If}{\pi r_o} \int_{-\pi r_o}^{\pi r_o} \frac{x - x'}{(x - x')^2 + (y - y')^2} \, dy' \tag{29b}$$

since $ds \cos \alpha = dy$, where ds is an element of arc length along the sheet. The total field can be obtained by adding the field of the wire to equations (28). If equations (25) are used the field components are:

$$\frac{H_x}{(8\pi p_o)^{1/2}} = \frac{1}{4f} \left[\frac{-2\eta}{\xi^2 + \eta^2} + \frac{2f}{\pi} \int_{-\pi}^{\pi} \frac{(\eta - \eta') \sin^2 \eta'}{(\xi \sin \eta' - \eta' \cos \eta')^2 + (\eta - \eta')^2 \sin^2 \eta'} \, d\eta' \right] \tag{30a}$$

$$\frac{H_y}{(8\pi p_o)^{1/2}} = \frac{1}{4f}\left[\frac{2\eta}{\xi^2 + \eta^2}\right.$$

$$\left. - \frac{2f}{\pi}\int_{-\pi}^{\pi} \frac{(\xi \sin\eta' - \eta'\cos\eta')\sin\eta'}{(\xi \sin\eta' - \eta'\cos\eta')^2 + (\eta - \eta')^2\sin^2\eta'}\, d\eta'\right] \quad (30b)$$

The field lines can be computed by integrating the equation

$$\frac{d\eta}{d\xi} = \frac{dy}{dx} = \frac{H_y}{H_x} \quad (31)$$

Equation (31) can now be solved by computing H_x and H_y from equations (30) and integrating numerically. The integrals in equations (30) are free from singularities except when the integral curve lies on the bounding sheath. In that case the denominators of the integrands vanish. Because of this difficulty, the integrals were split into three parts:

$$\int_{-\pi}^{\pi} \frac{(\eta - \eta')\sin^2\eta'}{(\xi \sin\eta' - \eta'\cos\eta')^2 + (\eta - \eta')\sin^2\eta'}\, d\eta'$$

$$= \int_{-\pi}^{\eta-\epsilon} \frac{(\eta - \eta')\sin^2\eta'}{(\xi \sin\eta' - \eta'\cos\eta')^2 + (\eta - \eta')^2\sin^2\eta'}\, d\eta'$$

$$+ \int_{\eta+\epsilon}^{\pi} \frac{(\eta - \eta')\sin^2\eta'}{(\xi \sin\eta' - \eta'\cos\eta')^2 + (\eta - \eta')^2\sin^2\eta'}\, d\eta' + K_1 \quad (32a)$$

$$\int_{-\pi}^{\pi} \frac{(\xi \sin\eta' - \eta'\cos\eta')\sin\eta'}{(\xi \sin\eta' - \eta'\cos\eta')^2 + (\eta - \eta')^2\sin^2\eta'}\, d\eta'$$

$$= \int_{-\pi}^{\eta-\epsilon} \frac{(\xi \sin\eta' - \eta'\cos\eta')\sin\eta'}{(\xi \sin\eta' - \eta'\cos\eta')^2 + (\eta - \eta')^2\sin^2\eta'}\, d\eta'$$

$$+ \int_{\eta+\epsilon}^{\pi} \frac{(\xi \sin\eta' - \eta'\cos\eta')\sin\eta'}{(\xi \sin\eta' - \eta'\cos\eta')^2 + (\eta - \eta')^2\sin^2\eta'}\, d\eta' + K_2 \tag{32b}$$

where

$$K_1 = \int_{\eta-\epsilon}^{\eta+\epsilon} \frac{(\eta' - \eta)\sin^2\eta'}{(\xi \sin\eta' - \eta'\cos\eta')^2 + (\eta - \eta')^2\sin^2\eta'}\, d\eta' \tag{32c}$$

$$K_2 = \int_{\eta-\epsilon}^{\eta+\epsilon} \frac{(\xi \sin\eta' - \eta'\cos\eta')\sin\eta'}{(\xi \sin\eta' - \eta'\cos\eta')^2 + (\eta - \eta')^2\sin^2\eta'}\, d\eta' \tag{32d}$$

The singularities are now contained in K_1 and K_2. They were then evaluated approximately as follows: The substitution

$$\eta' = \eta + \delta$$

was made in equations (32c and (32d), and linear terms in δ were retained. This approximation amounts to replacing the actual boundary in the neighborhood of $\eta' = \eta$ with a straight segment whose slope is equal to the boundary slope at η. The resulting integrals can then be evaluated analytically. Thus K_1 and K_2 were found to be approximately

$$K_1 \approx \frac{1}{2(B^2 + 1)} \log \frac{(A - \xi + B\epsilon)^2 + \epsilon^2}{(A - \xi - B\epsilon)^2 + \epsilon^2} - \frac{B}{B^2 + 1} \tan^{-1} \frac{B(A - \xi) + \epsilon(B^2 + 1)}{A - \xi}$$

$$+ \frac{B}{B^2 + 1} \tan^{-1} \frac{B(A - \xi) - \epsilon(B + 1)}{A - \xi} \tag{33a}$$

$$K_2 \approx \frac{B}{2(B^2+1)} \log \frac{(A-\xi+B\epsilon)^2+\epsilon^2}{(A-\xi-B\epsilon)^2+\epsilon^2} + \frac{1}{B^2+1} \tan^{-1} \frac{B(A-\xi)+\epsilon(B^2+1)}{A-\xi}$$

$$- \frac{1}{B^2+1} \tan^{-1} \frac{B(A-\xi)-\epsilon(B^2+1)}{A-\xi} \tag{33b}$$

where

$$A = \eta \cot \eta \tag{33c}$$

$$B = \cot \eta - \frac{\eta}{\sin^2 \eta} \tag{33d}$$

Equation (31) was then integrated numerically. An approximate field line was computed corresponding to each exact field line obtained previously. In every case except for the field line starting at the nose of the boundary, the starting point for the integration was chosen so that the exact and approximate curves coincided on the positive x axis. When integration was started precisely at the nose of the boundary, numerical difficulties arose. It was found, however, that integration could be started just inside the boundary. The starting value chosen was 0.99999 times the x coordinate of the nose. Small variations in the starting point did not affect the resulting field line appreciably. Results of the calculation are compared with the exact solution in figure 4 and are given in more detail in figure 5. In figure 5 the magnitude of the magnetic field is indicated by means of ticks. The magnetic field strengths indicated on the bounding field line were calculated just inside the boundary. Numerical results for coordinates and magnetic field components are given in table II. As in the exact case it was convenient to use polar coordinates. They are related to ξ and η by

$$\bar{r} = f(\xi^2 + \eta^2)^{1/2} \tag{34a}$$

$$\theta = \tan^{-1}\left(\frac{\eta}{\xi}\right) \tag{34b}$$

The components of the magnetic field, $H_{\bar{r}}$ and H_θ, are related to H_x and H_y by equations (24).

The magnetic flux passing between the nose of the boundary and any field line can be computed as follows. From equation (6b)

$$\bar{\psi} = \psi - \psi_N = \int_{x_N}^{x} H_y \, dx' \tag{35}$$

where x_N is the x coordinate of the boundary nose and x is any point in the field. Substituting from equation (25b) gives

$$\bar{\psi} = -4If \int_{\xi_N}^{\xi} \frac{H_y}{(8\pi p_o)^{1/2}} d\xi' \tag{36}$$

The integration was carried out numerically for each field line computed and the results are given in table II.

RESULTS AND DISCUSSION

An exact solution for the interaction of a neutral rarefied plasma stream with the magnetic field of a line current has been presented. Although the shape of the boundary has been obtained previously, the magnetic field is presented here for the first time. The method employed is applicable in part to many such two-dimensional problems. The magnetic field inside Ferraro's approximate boundary has also been determined. It follows from a comparison of the boundaries that the numerical value for f obtained by Ferraro is extremely close to the value one obtains by matching the approximate with the exact boundary at the nose. From figure 4 it can be seen that exact and approximate field lines which begin at the same point remain extremely close together in the upstream portion of the figure. In the downstream portion the most serious divergence between pairs of field lines is that between the exact bounding field line and the approximate field line which almost coincides with it at the nose. In this case the approximate field line forms a closed curve while the exact one goes to infinity in the negative x direction. Since the approximate field line is not altered significantly by slight variations in the starting point of the integration, it is concluded that this divergence is not due to a numerical difficulty but is inherent in the approximation. It can be seen from figures 3 and 5 (or tables I and II) that in the upstream part of the figure the magnetic field strengths on corresponding field lines are very nearly the same. The disagreement in the downstream part of the figure is due mainly to the divergence of the field lines themselves.

It has been shown above that the approximate field lines, with the exception of the one starting at the nose, agree with the exact ones to the same order (but opposite sense) that Ferraro's approximate boundary agrees with the exact one. The disagreement of the approximate field lines with the exact ones is a result of the disagreement of the approximate boundary with the exact one and not a result of the numerical computation scheme.

Ames Research Center
National Aeronautics and Space Administration
Moffett Field, Calif., Aug. 10, 1962

REFERENCES

1. Dungey, J. W.: Cosmic Electrodynamics. Cambridge, University Press, 1958.

2. Zhigulev, V. N., and Romishevskii, E. A.: Concerning the Interaction of Currents Flowing in a Conducting Medium with the Earth's Magnetic Field. Doklady Akad. Nauk SSSR, vol. 127, no. 5, 1959, pp. 1001-1004. (English translation: Soviet Physics - Doklady, vol. 4, no. 4, Feb. 1960, pp 859-862.)

3. Hurley, James: Interaction Between the Solar Wind and the Geomagnetic Field. New York University Report, March 1961.

4. Dungey, J. W.: The Steady State of the Chapman-Ferraro Problem in Two Dimensions. Jour. Geophys. Research, vol. 66, no. 4, April 1961, pp. 1043-1047.

5. Smith, E. J., Coleman, P. J., Judge, D. L., and Sonett, C. P.: Characteristics of the Extraterrestrial Current System: Explorer VI and Pioneer V. Jour. Geophys. Research, vol. 65, no. 6, June 1960, pp. 1858-1861.

6. Ferraro, V. C. A.: An Approximate Method of Estimating the Size and Shape of the Stationary Hollow Carved Out in a Neutral Ionized Stream of Corpuscles Impinging on the Geomagnetic Field. Jour. Geophys. Research, vol. 65, no. 12, Dec. 1960, pp. 3951-3953.

7. Hurley, James: Interaction of a Streaming Plasma With the Magnetic Field of a Line Current. Physics of Fluids, vol. 4, no. 1, Jan. 1961, pp. 109-111.

8. Beard, David B.: The Interaction of the Terrestrial Magnetic Field With the Solar Corpuscular Radiation. Jour. Geophys. Research, vol. 65, no. 11, Nov. 1960, pp. 3559-3568.

9. Spreiter, John R., and Briggs, Benjamin R.: Theoretical Determination of the Form of the Hollow Produced in the Solar Corpuscular Stream by Interaction With the Magnetic Dipole Field of the Earth. NASA TR R-120, 1961.

10. Panofsky, Wolfgang K. H., and Philips, Melba: Classical Electricity and Magnetism. Addison Wesley, 1955.

TABLE I.- EXACT SOLUTION FOR MAGNETIC FIELD LINES AND FIELD COMPONENTS INSIDE SHEATH

θ, deg	$\frac{1}{I}\bar{\psi} = 0$			$\frac{1}{I}\bar{\psi} = 0.25$			$\frac{1}{I}\bar{\psi} = 0.50$			$\frac{1}{I}\bar{\psi} = 1.0$		
	$\bar{r}$	$\frac{H_\theta}{\sqrt{8\pi p_o}}$	$\frac{H_{\bar{r}}}{\sqrt{8\pi p_o}}$	$\bar{r}$	$\frac{H_\theta}{\sqrt{8\pi p_o}}$	$\frac{H_{\bar{r}}}{\sqrt{8\pi p_o}}$	$\bar{r}$	$\frac{H_\theta}{\sqrt{8\pi p_o}}$	$\frac{H_{\bar{r}}}{\sqrt{8\pi p_o}}$	$\bar{r}$	$\frac{H_\theta}{\sqrt{8\pi p_o}}$	$\frac{H_{\bar{r}}}{\sqrt{8\pi p_o}}$
0	0.6931	1.0000	0.0000	0.6326	1.0666	0.0000	0.5759	1.1420	0.0000	0.4741	1.3244	0.0000
10	.6964	.9913	.0532	.6353	1.0579	.0524	.5782	1.1334	.0516	.4757	1.3159	.0501
20	.7063	.9654	.1042	.6436	1.0323	.1026	.5852	1.1080	.1010	.4804	1.2910	.0983
30	.7232	.9231	.1509	.6578	.9904	.1486	.5969	1.0666	.1464	.4885	1.2503	.1426
40	.7478	.8658	.1913	.6783	.9338	.1885	.6139	1.0106	.1858	.4999	1.1954	.1812
50	.7813	.7953	.2237	.7059	.8642	.2206	.6365	.9418	.2177	.5150	1.1280	.2127
60	.8252	.7140	.2466	.7416	.7839	.2435	.6655	.8625	.2407	.5339	1.0504	.2359
70	.8817	.6244	.2590	.7868	.6958	.2563	.7017	.7756	.2540	.5569	.9655	.2500
80	.9541	.5296	.2602	.8435	.6029	.2585	.7461	.6841	.2570	.5843	.8761	.2546
90	1.0472	.4330	.2500	.9140	.5084	.2500	.8000	.5913	.2500	.6162	.7855	.2500
100	1.1681	.3381	.2288	1.0015	.4161	.2315	.8646	.5007	.2336	.6527	.6969	.2368
110	1.3278	.2484	.1977	1.1098	.3294	.2042	.9410	.4157	.2091	.6935	.6133	.2161
120	1.5447	.1679	.1586	1.2430	.2521	.1705	1.0298	.3395	.1787	.7376	.5376	.1896
130	1.8512	.1003	.1144	1.4037	.1872	.1333	1.1294	.2748	.1449	.7836	.4720	.1592
140	2.3111	.0490	.0696	1.5898	.1370	.0966	1.2354	.2234	.1105	.8289	.4180	.1268
150	3.0716	.0164	.0309	1.7876	.1021	.0639	1.3390	.1856	.0781	.8702	.3765	.0940
160				1.9683	.0808	.0376	1.4275	.1605	.0492	.9035	.3472	.0618
170				2.0957	.0699	.0172	1.4875	.1465	.0236	.9252	.3300	.0306
180				2.1413	.0666	.0000	1.5087	.1420	.0000	.9328	.3244	.0000

θ, deg	$\frac{1}{I}\bar{\psi} = 1.5$			$\frac{1}{I}\bar{\psi} = 2.0$			$\frac{1}{I}\bar{\psi} = 3.0$			$\frac{1}{I}\bar{\psi} = 5.0$		
	$\bar{r}$	$\frac{H_\theta}{\sqrt{8\pi p_o}}$	$\frac{H_{\bar{r}}}{\sqrt{8\pi p_o}}$	$\bar{r}$	$\frac{H_\theta}{\sqrt{8\pi p_o}}$	$\frac{H_{\bar{r}}}{\sqrt{8\pi p_o}}$	$\bar{r}$	$\frac{H_\theta}{\sqrt{8\pi p_o}}$	$\frac{H_{\bar{r}}}{\sqrt{8\pi p_o}}$	$\bar{r}$	$\frac{H_\theta}{\sqrt{8\pi p_o}}$	$\frac{H_{\bar{r}}}{\sqrt{8\pi p_o}}$
0	.3869	1.5585	.0000	.3133	1.8591	.0000	.2014	2.7408	.0000	.0789	6.5912	.0000
10	.3879	1.5502	.0489	.3140	1.8510	.0479	.2017	2.7329	.0463	.0789	6.5835	.0445
20	.3912	1.5257	.0959	.3161	1.8268	.0939	.2026	2.7093	.0909	.0791	6.5605	.0876
30	.3965	1.4857	.1393	.3196	1.7874	.1365	.2041	2.6708	.1324	.0793	6.5230	.1279
40	.4041	1.4317	.1773	.3246	1.7341	.1740	.2061	2.6187	.1692	.0796	6.4722	.1640
50	.4140	1.3654	.2085	.3310	1.6688	.2051	.2087	2.5548	.2001	.0800	6.4097	.1948
60	.4262	1.2892	.2319	.3388	1.5937	.2288	.2118	2.4811	.2242	.0805	6.3375	.2194
70	.4408	1.2057	.2468	.3480	1.5113	.2443	.2154	2.4001	.2407	.0810	6.2578	.2371
80	.4577	1.1178	.2528	.3584	1.4244	.2513	.2193	2.3144	.2493	.0815	6.1731	.2474
90	.4769	1.0286	.2500	.3700	1.3360	.2500	.2236	2.2269	.2500	.0821	6.0861	.2500
100	.4981	.9409	.2390	.3825	1.2488	.2407	.2281	2.1401	.2429	.0827	5.9994	.2450
110	.5209	.8578	.2209	.3956	1.1658	.2243	.2326	2.0568	.2287	.0833	5.9156	.2327
120	.5446	.7818	.1968	.4089	1.0893	.2017	.2370	1.9795	.2079	.0838	5.8373	.2135
130	.5683	.7151	.1681	.4218	1.0216	.1742	.2412	1.9104	.1816	.0843	5.7667	.1881
140	.5908	.6592	.1365	.4338	.9643	.1429	.2450	1.8513	.1506	.0848	5.7060	.1572
150	.6105	.6152	.1031	.4440	.9188	.1090	.2481	1.8038	.1161	.0852	5.6569	.1219
160	.6260	.5837	.0689	.4520	.8858	.0735	.2505	1.7691	.0788	.0854	5.6208	.0832
170	.6359	.5648	.0345	.4570	.8658	.0369	.2520	1.7479	.0398	.0856	5.5987	.0422
180	.6394	.5585	.0000	.4587	.8591	.0000	.2525	1.7408	.0000	.0857	5.5912	.0000

TABLE II.- APPROXIMATE SOLUTION FOR MAGNETIC FIELD LINES AND FIELD COMPONENTS INSIDE SHEATH

θ, deg	Approximate sheath			$\frac{1}{I}\bar{\Psi} \approx 0$			$\frac{1}{I}\bar{\Psi} = 0.2430$		
	$\bar{r}$	$\frac{H_\theta}{\sqrt{8\pi p_o}}$	$\frac{H_{\bar{r}}}{\sqrt{8\pi p_o}}$	$\bar{r}$	$\frac{H_\theta}{\sqrt{8\pi p_o}}$	$\frac{H_{\bar{r}}}{\sqrt{8\pi p_o}}$	$\bar{r}$	$\frac{H_\theta}{\sqrt{8\pi p_o}}$	$\frac{H_{\bar{r}}}{\sqrt{8\pi p_o}}$
0	0.6931	0.9724	0.0000	0.6931	0.9727	0.0000	0.6326	1.0382	0.0000
10	.6960	.9621	.0465	.6961	.9630	.0468	.6351	1.0304	.0469
20	.7067	.9372	.0911	.7051	.9365	.0922	.6427	1.0071	.0918
30	.7251	.8966	.1318	.7204	.8990	.1329	.6557	.9693	.1328
40	.7521	.8416	.1671	.7426	.8516	.1712	.6742	.9182	.1683
50	.7888	.7738	.1954	.7728	.7853	.2001	.6990	.8556	.1968
60	.8373	.6956	.2155	.8115	.7148	.2194	.7306	.7843	.2177
70	.9003	.6093	.2264	.8588	.6277	.2095	.7695	.7043	.2240
80	.9818	.5180	.2277	.9146	.5527	.2159	.8166	.6238	.2260
90	1.0877	.4248	.2192	.9844	.4741	.2139	.8732	.5427	.2204
100	1.2272	.3328	.2015	1.0705	.3955	.2018	.9408	.4633	.2070
110	1.4147	.2454	.1756	1.1760	.3207	.1814	1.0202	.3886	.1868
120	1.6746	.1659	.1431	1.3036	.2530	.1550	1.1119	.3210	.1615
130	2.0510	.0976	.1067	1.4551	.1947	.1253	1.2148	.2625	.1331
140	2.6323	.0432	.0697	1.6292	.1472	.0950	1.3250	.2146	.1036
150	3.6257	.0052	.0366	1.8179	.1110	.0665	1.4347	.1777	.0750
160				2.0001	.0858	.0413	1.5313	.1519	.0482
170				2.1392	.0711	.0195	1.5989	.1368	.0234
180				2.1923	.0662	.0000	1.6233	.1318	.0000
	$\frac{1}{I}\bar{\Psi} = 0.4866$			$\frac{1}{I}\bar{\Psi} = 0.9753$			$\frac{1}{I}\bar{\Psi} = 1.4658$		
0	.5759	1.1140	.0000	.4741	1.2969	.0000	.3869	1.5315	.0000
10	.5780	1.1062	.0462	.4755	1.2893	.0449	.3878	1.5241	.0438
20	.5844	1.0832	.0904	.4799	1.2667	.0880	.3908	1.5019	.0859
30	.5951	1.0458	.1309	.4872	1.2301	.1276	.3957	1.4659	.1248
40	.6105	.9953	.1661	.4975	1.1806	.1621	.4025	1.4173	.1588
50	.6308	.9334	.1944	.5111	1.1200	.1903	.4114	1.3578	.1868
60	.6565	.8626	.2150	.5279	1.0505	.2109	.4223	1.2893	.2078
70	.6879	.7847	.2250	.5481	.9745	.2232	.4351	1.2145	.2211
80	.7256	.7041	.2277	.5717	.8950	.2276	.4499	1.1359	.2268
90	.7700	.6230	.2226	.5988	.8146	.2242	.4664	1.0561	.2249
100	.8217	.5438	.2100	.6292	.7358	.2136	.4845	.9776	.2159
110	.8808	.4691	.1909	.6624	.6613	.1967	.5036	.9030	.2006
120	.9465	.4014	.1668	.6976	.5932	.1746	.5314	.8200	.1798
130	1.0173	.3426	.1394	.7335	.5333	.1487	.5427	.7736	.1549
140	1.0896	.2939	.1105	.7682	.4832	.1203	.5609	.7222	.1268
150	1.1582	.2561	.0815	.7994	.4437	.0906	.5767	.6814	.0965
160	1.2157	.2294	.0534	.8243	.4153	.0604	.5890	.6518	.0649
170	1.2544	.2135	.0263	.8405	.3982	.0302	.5969	.6339	.0326
180	1.2681	.2083	.0000	.8461	.3926	.0000	.5996	.6279	.0000
	$\frac{1}{I}\bar{\Psi} = 1.9579$			$\frac{1}{I}\bar{\Psi} = 2.9462$			$\frac{1}{I}\bar{\Psi} = 4.9336$		
0	.3133	1.8326	.0000	.2014	2.7151	.0000	.0789	6.5664	.0000
10	.3139	1.8253	.0429	.2017	2.7079	.0416	.0789	6.5594	.0401
20	.3158	1.8035	.0842	.2025	2.6866	.0817	.0791	6.5387	.0789
30	.3191	1.7680	.1224	.2038	2.6520	.1189	.0793	6.5049	.1152
40	.3235	1.7201	.1561	.2057	2.6051	.1520	.0795	6.4591	.1478
50	.3293	1.6614	.1840	.2080	2.5476	.1799	.0799	6.4028	.1756
60	.3363	1.5938	.2053	.2108	2.4812	.2016	.0803	6.3376	.1978
70	.3444	1.5198	.2193	.2140	2.4083	.2167	.0808	6.2658	.2138
80	.3536	1.4419	.2260	.2175	2.3312	.2247	.0813	6.1894	.2232
90	.3637	1.3625	.2252	.2213	2.2523	.2255	.0818	6.1108	.2257
100	.3745	1.2842	.2175	.2252	2.1741	.2195	.0823	6.0325	.2213
110	.3857	1.2094	.2034	.2291	2.0989	.2070	.0828	5.9569	.2103
120	.3970	1.1403	.1837	.2411	1.9566	.1848	.0833	5.8861	.1930
130	.4079	1.0788	.1594	.2367	1.9664	.1650	.0838	5.8224	.1701
140	.4178	1.0264	.1314	.2399	1.9127	.1371	.0842	5.7675	.1423
150	.4263	.9846	.1007	.2426	1.8695	.1058	.0845	5.7230	.1104
160	.4329	.9541	.0681	.2447	1.8379	.0719	.0847	5.6904	.0754
170	.4370	.9356	.0343	.2459	1.8186	.0364	.0849	5.6704	.0382
180	.4384	.9293	.0000	.2464	1.8121	.0000	.0849	5.6636	.0000

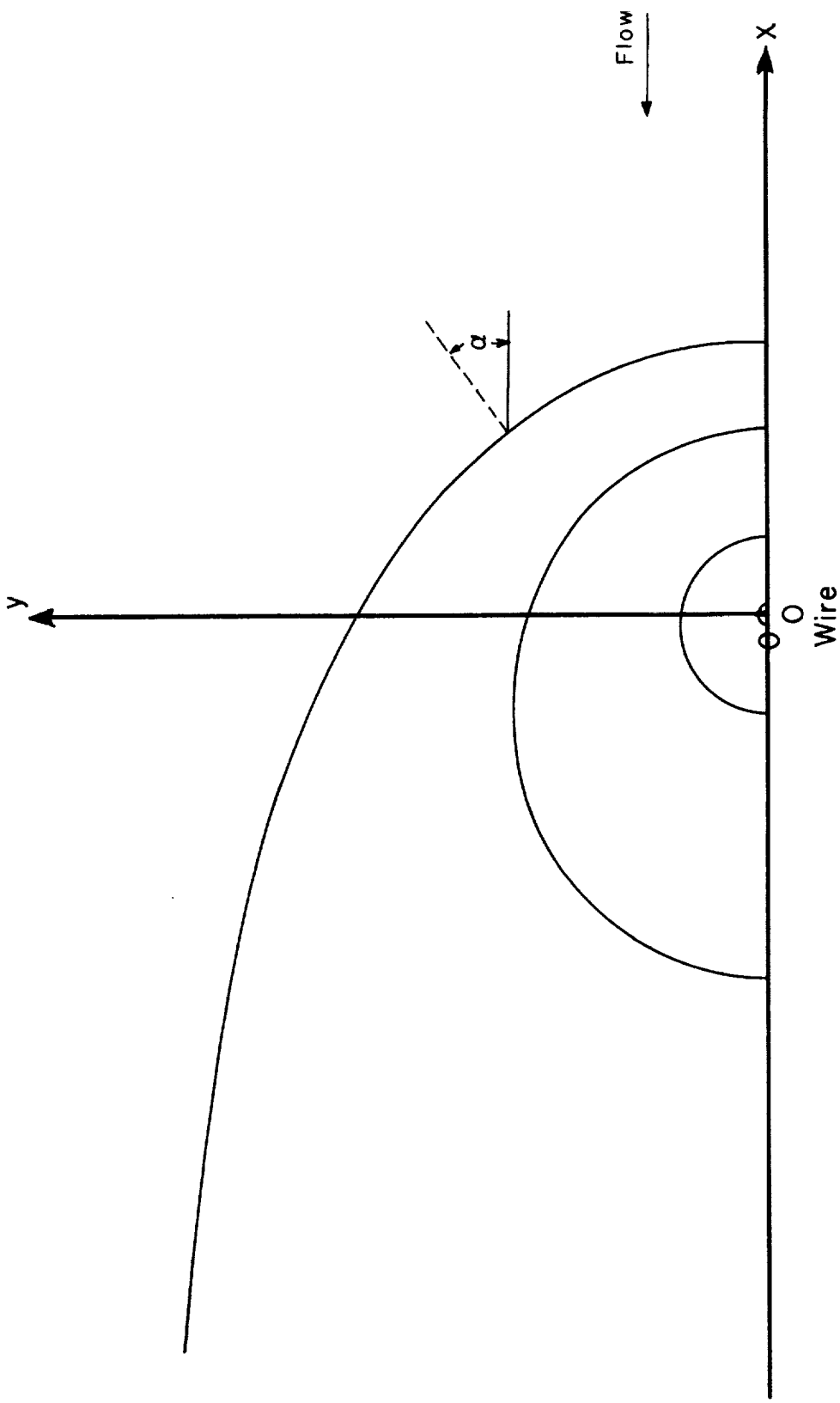

Figure 1.- View of field lines and coordinate system.

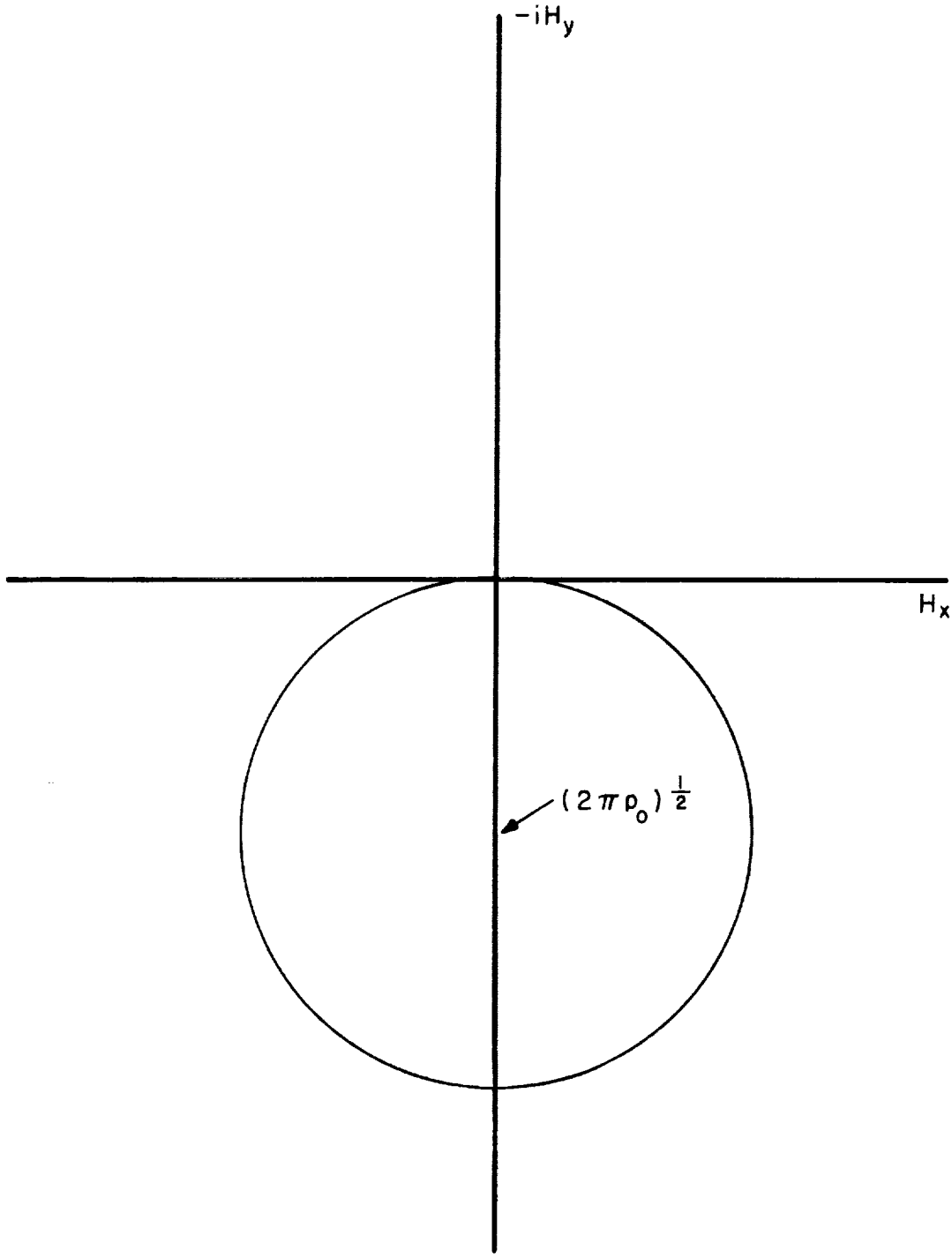

Figure 2.- The sheath in the magnetic plane.

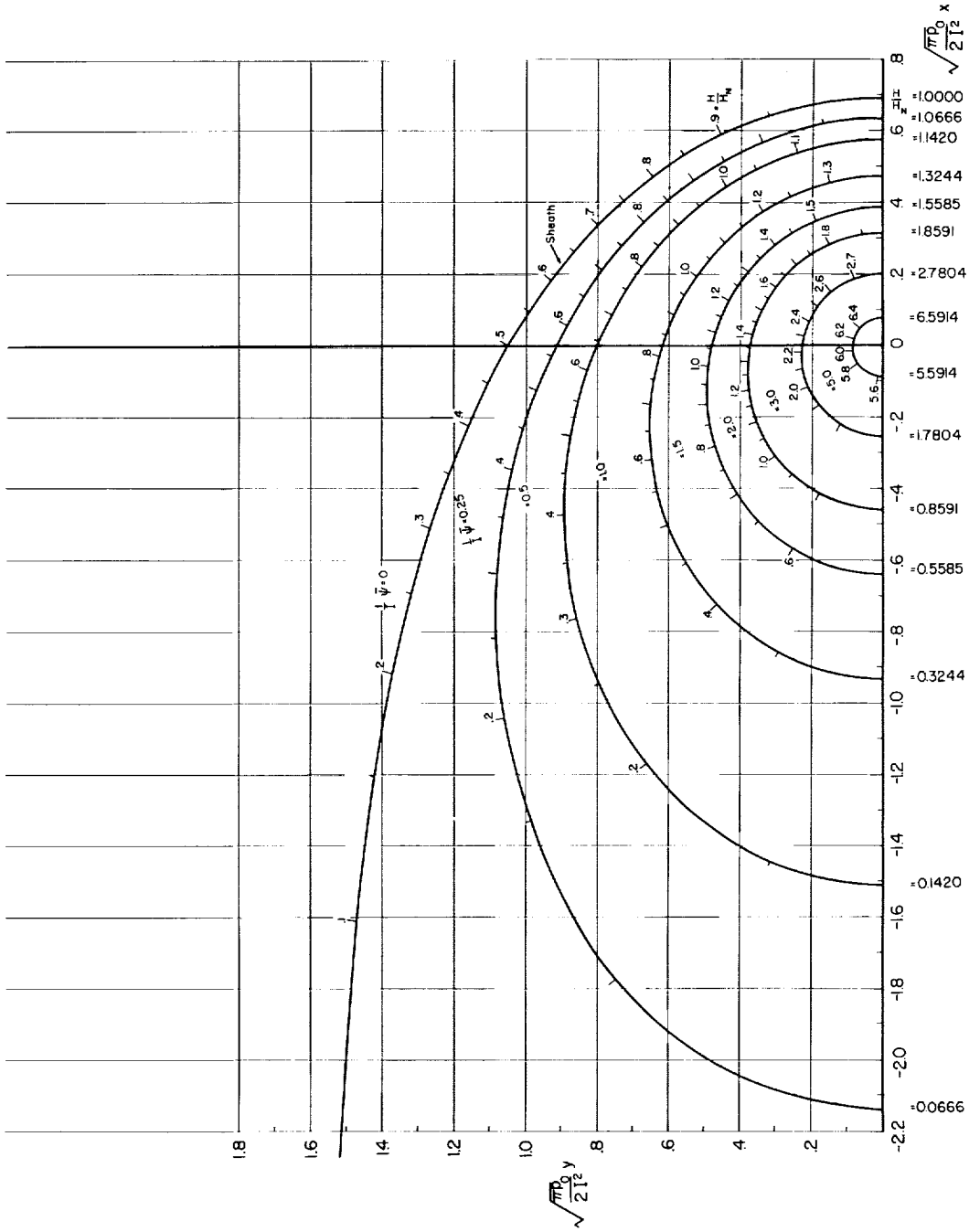

Figure 3.- Exact solution for magnetic field inside sheath.

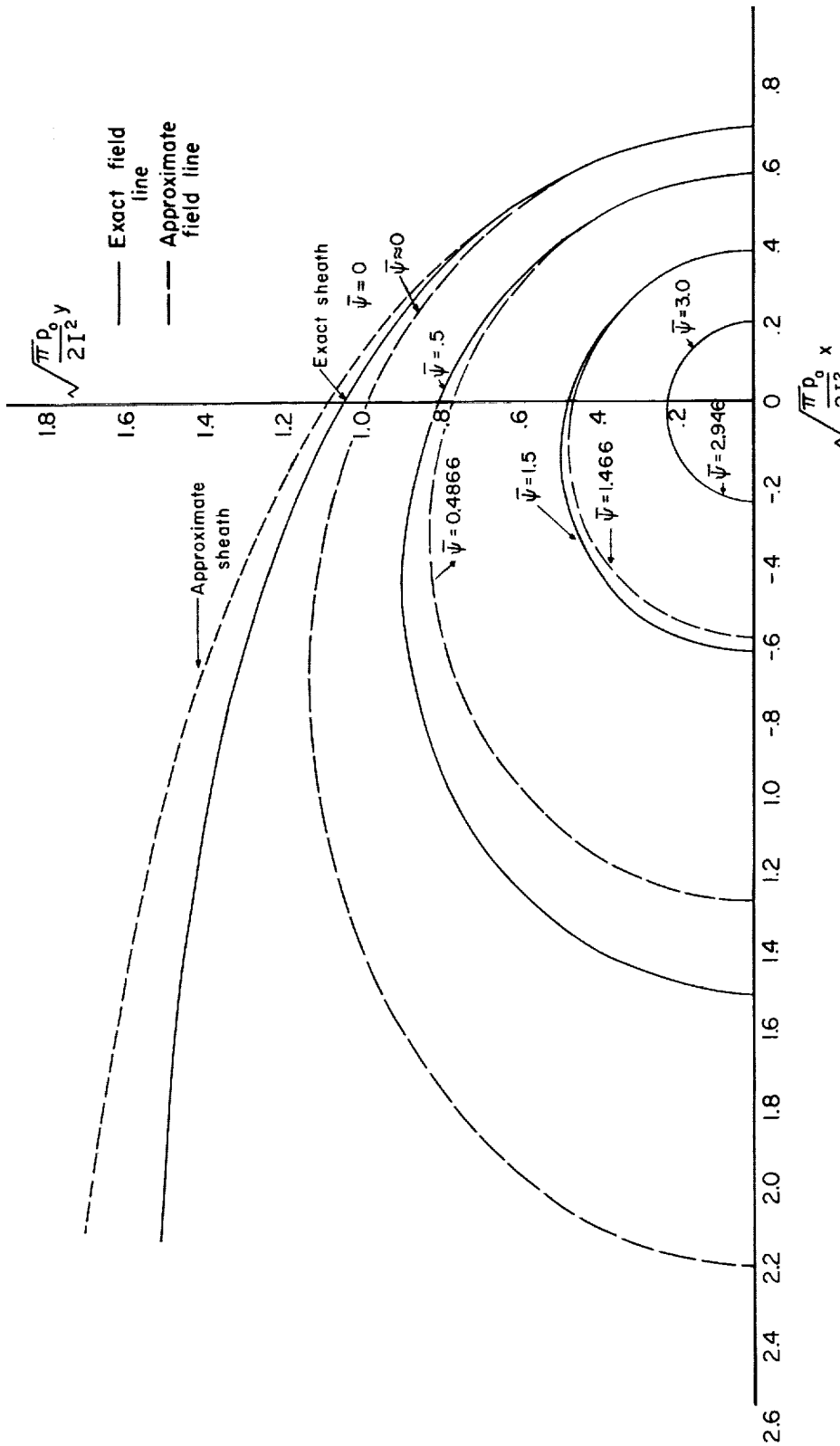

Figure 4.- Comparison of exact and approximate solutions for magnetic field inside sheath.

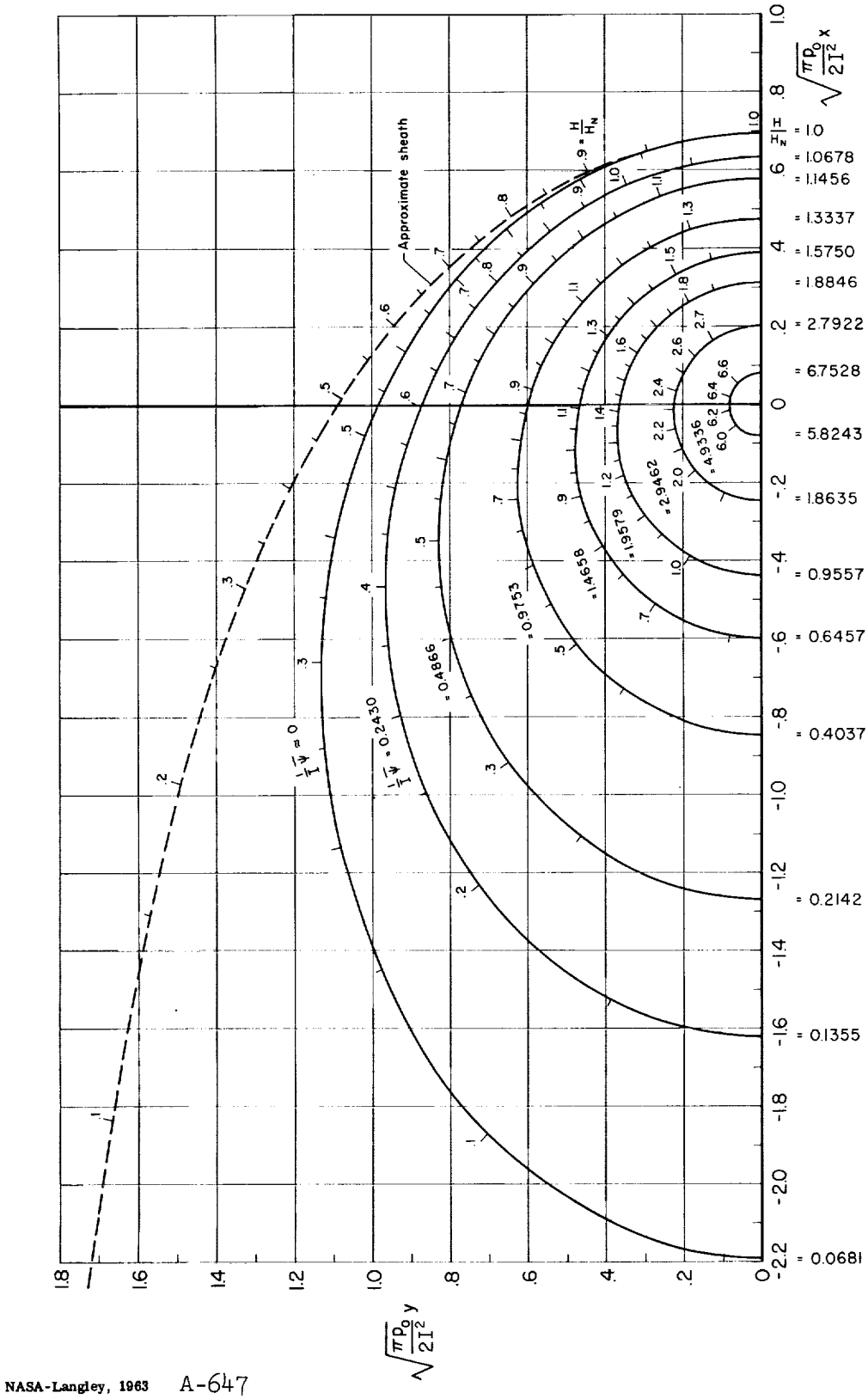

NASA-Langley, 1963 A-647

Figure 5.- Approximate solution for magnetic field inside sheath.